

RESEARCH ARTICLE

Acid-assisted leaching of iron and manganese from Sri Lankan laterite: a potential source of alumina production

IA Goonetilleke¹, HCS Subasinghe¹, AS Ratnayake^{1*} and DT Jayawardana²

¹ Department of Applied Earth Sciences, Faculty of Applied Sciences, Uva Wellassa University, Badulla.

² Faculty of Applied Sciences, University of Sri Jayawardenepura, Gangodawila, Nugegoda.

Submitted: 02 September 2020; Revised: 13 December 2020; Accepted: 26 March 2021

Abstract: Laterites are of great interest for industrial applications. This study is focussed on determining optimum conditions (i.e. pH, temperature, and sonication time) for leaching Fe and Mn from Sri Lankan laterite. Physicochemical parameters, atomic absorption spectroscopy (AAS), X-ray diffraction (XRD), and Fourier-transform infrared (FTIR) spectroscopic analyses were performed. Different solutions were prepared for a pH range from 1 to 10, temperature from 40 °C to 100 °C, and sonication time from 10 min to 60 min. Elemental concentrations of the filtrates were used to determine the optimum conditions. Fe and Mn leaching efficiencies decreased with increasing pH from 1 to 5. The solution of pH 1 indicated the maximum leaching capacities of Fe (17.69 ppm) and Mn (2.05 ppm). Fe and Mn leaching efficiencies almost exhibited a positive correlation with temperature. The maximum leaching concentrations were observed after 15 min of sonication. Therefore, the optimum conditions for leaching both Fe and Mn were determined as pH 1 at 60 °C temperature after 15 minutes of sonication. Precipitates of treated samples were characterised using XRD and FTIR to determine changes compared to the raw sample. XRD results identified the crystalline phases, and thereby chemical composition of raw laterite can be discovered by the software as goethite and hematite as main Fe-rich minerals. The raw laterite was also associated with gibbsite, kaolinite, and quartz. However, weak reflections of hematite were observed in the XRD spectra of treated samples. FTIR observations suggested alteration of functional groups (e.g. the disappearance of Fe—O bond) in acid leached and sonicated samples. Consequently, FTIR and XRD results also confirmed the acid-leaching capacity of Sri Lankan laterite.

Keywords: Acid leaching, laterite, metal removal, value addition.

INTRODUCTION

Laterite is a common surficial/near surficial product of long-lasting and intensive tropical rock weathering and oxidation present in tropical countries such as Sri Lanka (Dahanayake, 1982; Pham *et al.*, 2020). According to Persons (2012), 'laterite is a stone of a thousand uses'. The most fundamental application of laterites is as a building material. Many economically important metallic elements (e.g. Al, Fe, Mn, Ni) are present in laterites (Maiti *et al.*, 2012; Çetintaş & Bingöl, 2020). Therefore, the extraction of these valuable components has been the focus of many researchers. For example, minor elements such as Zn, Cu, Ni, Cd, and Pb are present in Sri Lankan laterite (Nayanthika *et al.*, 2018). Furthermore, Sri Lankan laterites have been used in the synthesis of pure hematite nanoparticles as superior adsorption dyes (Dissanayake *et al.*, 2019).

Metals and metal oxides present in laterites can be leached using acids, and thus enhance the Al content (Nasab *et al.*, 2020). Bauxite and sillimanite are the globally prominent raw materials for the extraction of alumina and Al metal (Perks & Mudd, 2019). Alumina has many primary and advanced applications (The

* Corresponding author (as_ratnayake@uwu.ac.lk;  <https://orcid.org/0000-0001-7871-2401>)



This article is published under the Creative Commons CC-BY-ND License (<http://creativecommons.org/licenses/by-nd/4.0/>). This license permits use, distribution and reproduction, commercial and non-commercial, provided that the original work is properly cited and is not changed in anyway.

Aluminium Association, 2020). However, the availability of bauxite and sillimanite resources are limited. The industries utilising alumina as raw materials (e.g. cement industry) are urged to go for alternatives such as laterites and lateritic soils that are composed of Al_2O_3 (Moutei *et al.*, 2018). Consequently, laterites have been leached to obtain metals such as nickel and cobalt, and to enhance the workability of laterite as a source of alumina (Goswami & Mahanta, 2007; Liu *et al.*, 2010; Ayanda *et al.*, 2011; Ilyas *et al.*, 2020). Leaching and charging behaviour of laterites are strongly dependent on the pH (Pham *et al.*, 2020). However, complex mineralogy and limited application of existing technologies have caused difficulties in the processing of laterites for value addition (Nasab *et al.*, 2020).

Sri Lankan laterite is typically yellow, deep mottled red or reddish-brown ferruginous earth with many vesicular and botryoidal structures (Dahanayake, 1982). The mineralogical composition of Sri Lankan laterite is mainly composed of goethite, hematite, gibbsite, quartz, and clay minerals (Herath & Pathirana, 1983). However, the value addition potential of Sri Lankan laterites has rarely been focussed in the literature. Therefore, the current study is mainly focussed on investigating the metal leaching characteristics of Sri Lankan laterite. In this study, the authors investigated the optimum conditions such as pH, temperature, and sonication time for leaching iron and manganese from Sri Lankan laterite.

METHODOLOGY

Sample collection and powder sample preparation

The representative laterite samples were collected from a quarry site in Horana-Millaniya (global position system coordinates: 6°38'59"N 80°00'48"E) in the South-western Highland Complex of Sri Lanka. Samples were collected from about 1.50 m depth from the surface. Laterite samples were milled using a vertical planetary ball mill (Tencan XQM-0.4A, Japan) and sieved using a British standard sieve shaker to obtain the particles below 63 μm .

Physicochemical analysis of raw laterite

The wet and dry weight of raw laterite was measured at room temperature, and after heating at 105 °C for 24 h, respectively. Moisture content was calculated by

the difference between wet and dry weights to the initial wet weight.

About 5 g of the sample was ignited at 550 °C for 24 h using a Protherm-PLF 140/5 muffle furnace to remove organic matter. The sample was then reheated at 1050 °C for 2 h in the muffle furnace to evolve carbon dioxide from carbonate. Loss on ignition ($\text{LOI}_{1050} \text{ } ^\circ\text{C}$) was calculated by the difference between dry weight and ignited weight at 1050 °C to the dry weight (Heiri *et al.*, 2001).

Powdered raw laterite (< 63 μm) was oven-dried at 80 °C for 120 min. About 5 g of raw laterite was suspended in distilled water with 1:10 soil suspension ratio, and pH value was measured using an Edge® Multiparameter pH Meter - HI2020.

Determination of optimum conditions (pH range, temperature and sonication time)

(a) Raw laterite (5 g, particles < 63 μm and oven-dried at 80 °C for 120 min) was suspended in 50 mL of distilled water. Suspension solutions were prepared from pH 1 to 10 at room temperature. The pH of the solution was adjusted by adding aqueous HCl or aqueous NaOH dropwise. The mixture was filtered after 30 min. The filtrates and precipitates were collected. The precipitates were washed with distilled water to remove unconsumed acid/base and oven-dried at 80 °C for 60 min.

(b) Powdered and dried laterite (5 g) samples were suspended in 50 mL of distilled water to determine the optimum temperature. The pH values of the solutions were adjusted by adding 1 M HCl drop wise. After the determination of optimum pH range, pH 1 solutions were considered for further evaluation. The solutions were heated for 60 min at different temperatures of 40, 60, 80, and 100 °C in a water bath. The filtrate and the precipitate were collected after filtration.

(c) Powdered and dried laterite (5 g) samples were suspended in 50 mL of distilled water at room temperature (27 °C) to determine the optimum sonication time. The pH values were adjusted by drop wise addition of 1 M HCl. The pH 1 solution series was used to determine sonication time. The mixtures were sonicated for 10, 15, 30, 45 and 60 min using Rocker ultrasonic cleaner sonicator (Soner 206) at room temperature at a frequency of 53 kHz. The mixtures were filtered, and the filtrate and precipitate were collected.

Sample characterisation of raw and treated laterite samples

Atomic absorption spectroscopic (AAS) analysis

Raw laterite (5 g, particles < 63 μm and oven-dried at 80 $^{\circ}\text{C}$ for 2 h) was dissolved in 50 mL of distilled water and stirred for 30 min. Then, the mixture was filtered and the filtrate was collected to determine the water solubility of iron (Fe), cadmium (Cd), and manganese (Mn) in raw laterite.

Similarly, the filtrates of treated laterite were also collected to determine the leaching concentrations of Fe, Cd, and Mn. Concentrations of Fe, Cd, and Mn in the raw and treated samples were measured using Varian AA240 atomic absorption spectrometer, after calibrating the instrument linearly using relevant standards of known concentrations.

Fourier-transform infrared (FTIR) analysis

KBr pellet method was used to analyse the samples. The powdered samples were mixed with potassium bromide (KBr) at 1:10. The FTIR grade dried KBr (assay $\geq 99\%$) was used. A pellet (1 mm in thickness and 7 mm in diameter) was prepared for KBr/powdered sample mixture using a hand press pelletiser. The pellets of raw and treated (precipitate) laterite were placed directly in the beam of Bruker Alpha spectrophotometer over the range of 500–4000 cm^{-1} .

X-ray diffraction (XRD) analysis

The untreated and treated precipitates of laterite samples were finely powdered. These samples were analysed via powder X-Ray Diffraction (XRD) method using Rigaku Ultima IV X-ray diffractometer with $\text{Cu K}\alpha$ radiation ($\lambda=1.54$) at 40 kV and 30 mA. The diffractogram was recorded with a scanning rate of 0.02 $^{\circ}$ /s in a 2θ range from 10 $^{\circ}$ to 60 $^{\circ}$.

RESULTS AND DISCUSSION

Physicochemical parameters of raw laterite

The average pH of powdered laterite suspension in water was 5.69. Therefore, 1 M HCl and 1 M NaOH were used to prepare solutions of pH below 5.69 and pH above 5.69, respectively. The moisture content and $\text{LOI}_{1050}^{\circ}\text{C}$ values of raw laterite samples were 15.80 % and 16.56 %, respectively. $\text{LOI}_{1050}^{\circ}\text{C}$ value indicates

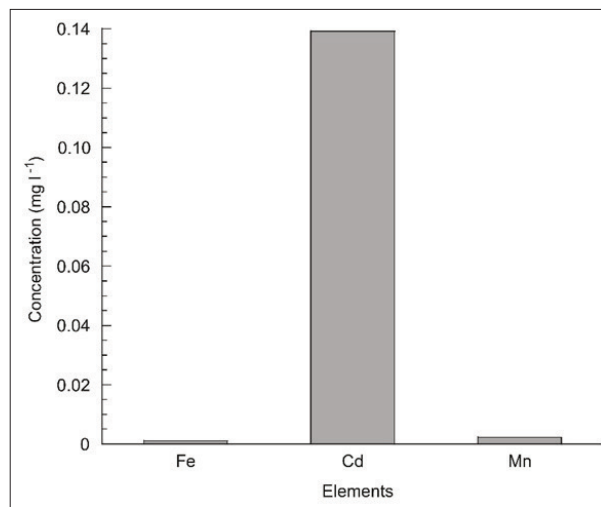


Figure 1: Concentration of Fe, Cd, and Mn ions present in water suspensions of powdered raw laterite

relatively high carbonate values for the raw laterite. In addition, raw laterite shows a higher abundance of Cd in filtrates relative to Fe and Mn (Figure 1). Consequently, Cd can be easily leached from laterite than Fe and Mn under normal soil pH conditions.

The geochemistry of laterites and lateritic soils significantly varies based on the location, climatic conditions, and depth. Layer thickness, geochemistry, and ore mineralogy of lateritic soils are determined by the degree of prolonged chemical weathering process. Laterites and their derivative soils contain SiO_2 , Al_2O_3 , Fe_2O_3 , and metals such as K, Mg, Ca, Ni, Co, Mn, Cd, and Ti (Dissanayake, 1980; Gleeson *et al.*, 2004; Fan & Gerson, 2011; Nayanthika *et al.*, 2018).

Determination of optimum conditions for the leaching of Fe and Mn from laterite

Effective pH range

Figure 2 shows variations in ion leaching capacities of selected elements with pH. Accordingly, the Fe leaching concentration decreases suddenly with increasing pH values from 1 to 2 (Figure 2). Then, Fe leaching concentration slightly decreases with increasing pH from 1 to 5. However, Fe concentrations are almost constant in pH values above 6 (Figure 2). Therefore, pH of 1 provides the highest leaching potential for Fe (17.69 ppm) with an enrichment factor of 17,690 compared to water solubility.

Mn leaching efficiency also decreases gradually with increasing pH from 1 to 5 (Figure 2). Clear variations of Mn concentrations were not observed in pH values above 6 (Figure 2). Therefore, Mn can be leached under low pH conditions (Figure 2). However, Cd dissolution concentration gradually increases from pH 1 to 10 (Figure 2). This suggests that Cd can be effectively leached under basic conditions, and the effective pH is 7 (0.18 ppm in Figure 2). Therefore, Cd does not leach well with 1 M HCl at any pH value, though it leaches in water.

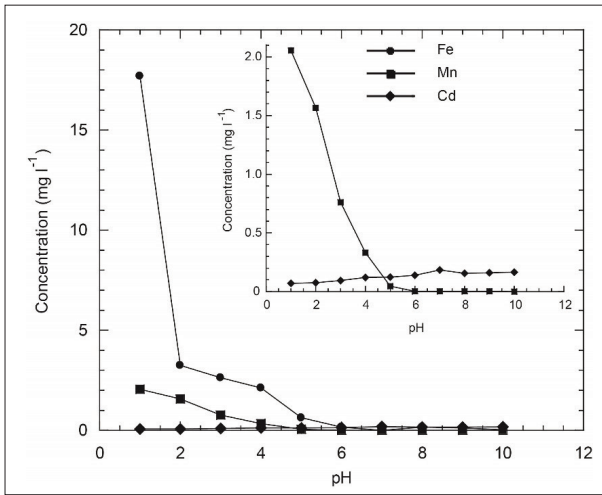


Figure 2: Variation of Fe, Mn, and Cd leaching concentrations with pH

Determination of optimum temperature

Figure 3 shows variations of Fe and Mn ions leaching concentrations with temperature in pH 1 solutions. Fe and Mn concentrations gradually increase with temperature (Figure 3). Therefore, temperature has a positive relationship with the leaching efficiency of Fe and Mn from laterite. The Fe leaching concentration at 40 °C is 17.11 ppm with an enrichment factor of 17,110. However, Fe concentration increases up to 19.04 ppm at 60 °C with an enrichment factor of 19,040 (Figure 3). Similarly, Mn leaching concentration slightly increases with temperature from 3.11 ppm (40 °C; enrichment factor: 1,555) to 3.18 ppm (60 °C; enrichment factor: 1,590). According to Figure 3, the highest leaching capacity can be estimated at over 100 °C. However, HCl evaporates at higher temperatures (Li *et al.*, 2012).

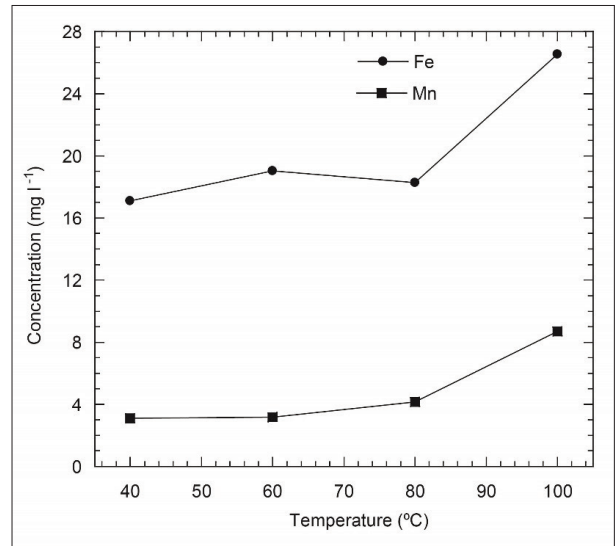


Figure 3: Variation of Fe and Mn leaching concentrations with temperature for pH 1 solutions

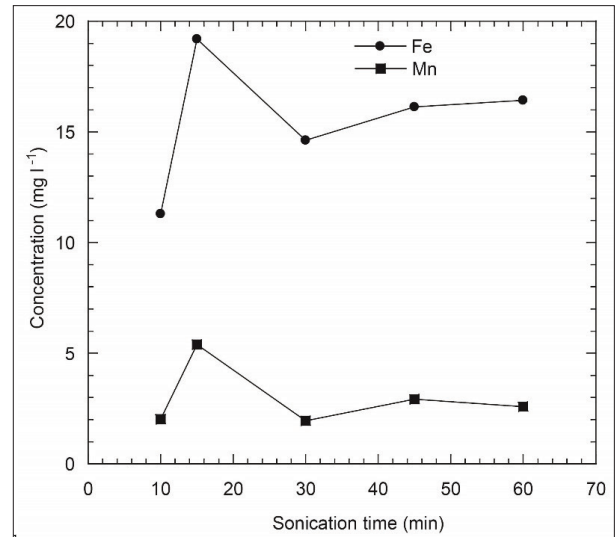


Figure 4: Variation of Fe and Mn leaching concentrations with sonication time for pH 1 solutions

Moreover, heating adds additional operational costs. Therefore, industries prefer to maintain the temperature around 60 °C for leaching elements from raw materials (Patermarakis & Paspaliaris, 1989).-

Determination of optimum sonication time

Figure 4 shows variations of Fe and Mn ion leaching concentrations with sonication time in pH 1 solutions. Fe and Mn ion leaching concentrations enhances with increasing sonication time from 10 min to 15 min (Figure 4). The highest Fe (19.19 ppm, enrichment factor: 19,190) and Mn (5.39 ppm; enrichment factor: 2,695) ions leaching concentrations can be observed in solutions sonicated for 15 min. In contrast, the maximum leaching concentrations under the influence of temperature (Fe concentration = 26.56 ppm and Mn concentration = 8.69 ppm at 100 °C in Figure 4) are higher than the influence of sonication time (Fe concentration = 19.19 ppm and Mn concentration = 5.39 ppm) at 15 min (Figure 4). However, sonication is preferred compared to heating in industrial applications (Kyllönen *et al.*, 2004).

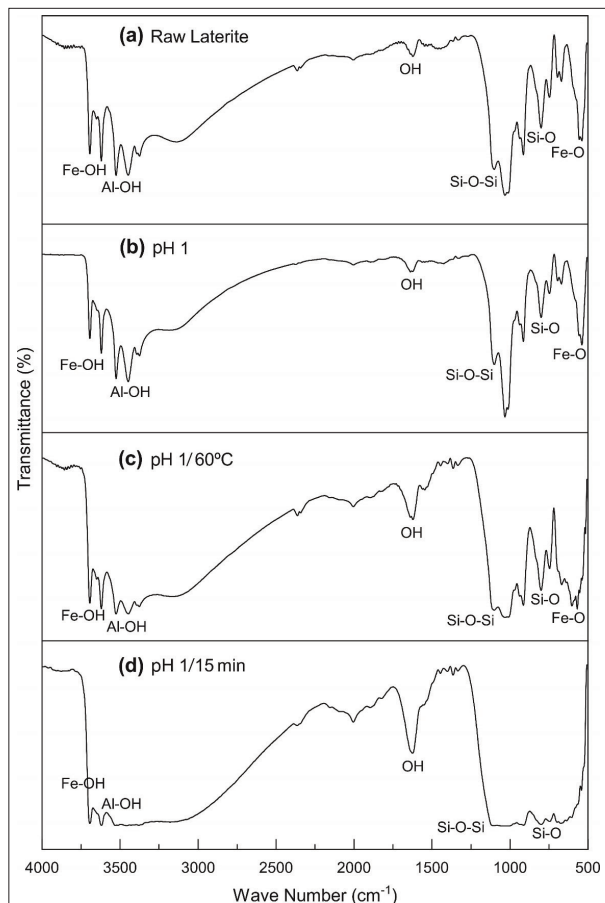


Figure 5: FTIR spectra of (a) untreated laterite sample, (b) acid leached (pH 1 solutions), (c) acid leached and heated (pH 1/60°C), and (d) acid leached and sonicated (pH 1/15 min) samples.

FTIR observations

The untreated laterite sample shows IR transmittance peaks for Fe, Al, and silicon oxide/hydroxide bonds (Figure 5a). For example, IR transmittance within the range 3300–3700 cm^{-1} (Figure 5) indicates hydroxyl groups and inner hydroxyl groups of laterites (Nayanthika *et al.*, 2018). Hydroxide groups of Fe, Al, and Si minerals are attributed to transmittance from 3370–3405 cm^{-1} . The transmission band around 3500 cm^{-1} indicates Al—OH stretching vibrations (Rathore *et al.*, 2016). Furthermore, 914 cm^{-1} and 801 cm^{-1} peaks (Figure 5) indicate Al—OH bending and Fe—OH stretching vibrations, respectively (Mitra *et al.*, 2016). In contrast, 1032 cm^{-1} peak suggests Si—O—Si stretching present in clay minerals (Rathore *et al.*, 2016). FTIR transmittance bands at 672 cm^{-1} and 536 cm^{-1} (Figure 5) correspond to Si—O bond in quartz and Fe—O bond in hematite, respectively (Mitra *et al.*, 2016; Rathore *et al.*, 2016).

The peaks corresponding to iron oxides such as Fe—OH (801 cm^{-1}) and Fe—O (536 cm^{-1}) are recorded in acid leached samples (pH 1 and pH 2 solutions) (Figure 5b), and acid leached and heated (pH 1/60°C) samples (Figure 5c). Therefore, it suggests that iron oxides remain in the precipitate after low pH acid leaching, and acid leaching at elevated temperatures (Figure 5b, c). Similarly, the peak corresponding to iron hydroxide (Fe—OH) can be observed in the acid leached and sonicated (pH 1/15 min) sample (Figure 5d). However, the peak corresponding to Fe—O bond in hematite has disappeared in the acid leached and sonicated (pH 1/15 min) sample (Figure 5d). Therefore, the combination of acid leaching and sonication can be identified as the most effective method for Fe leaching from laterite samples.

XRD observations

Figure 6a shows that raw laterite indicates the presence of Fe-rich secondary minerals such as goethite substituted with Al ($(\sim\text{Fe}_{0.9}\text{Al}_{0.1})\text{O}(\text{OH})$), hematite (Fe_2O_3), and Al-rich secondary minerals such as gibbsite ($\text{Al}(\text{OH})_3$). Kaolinite indicates the presence of clay minerals in laterite (Figure 6). Besides, goethite can occur in laterite as a weathering product of Fe-bearing minerals and as a direct precipitated agent from Fe-containing solutions (Mohapatra *et al.*, 2008). Goethite is metastable under a wide range of environmental conditions and temperatures (Cornell *et al.*, 1975) and has lower dissolution with 1M HCl than hematite (Cornell & Giovanoli, 1993). Consequently, the minor changes in peak positions and the increment of intensity in treated samples indicate that the Al-rich goethite in raw laterite has been converted to

gibbsite after leaching, thus enhancing the Al content in the samples (Figure 6).

The occurrence of quartz peaks in raw laterite suggests the presence of silicate minerals as impurities (Figure 6). Quartz in laterite can be coated with Fe-oxides such as hematite. In addition, the reduction of the number of hematite peaks after treatment indicates that raw laterite has been successfully leached, liberating Fe ions into the solution (Figure 6). However, the remaining hematite peaks in the treated samples suggest the presence of small amount of Fe even after treatment. Thus, acid leached (pH 1 solutions), acid leached and heated (pH 1/60°C), and acid leached and sonicated (pH 1/15 min) samples recorded more gibbsite peaks suggesting successful Al enhancement (Figure 6b, c, d).

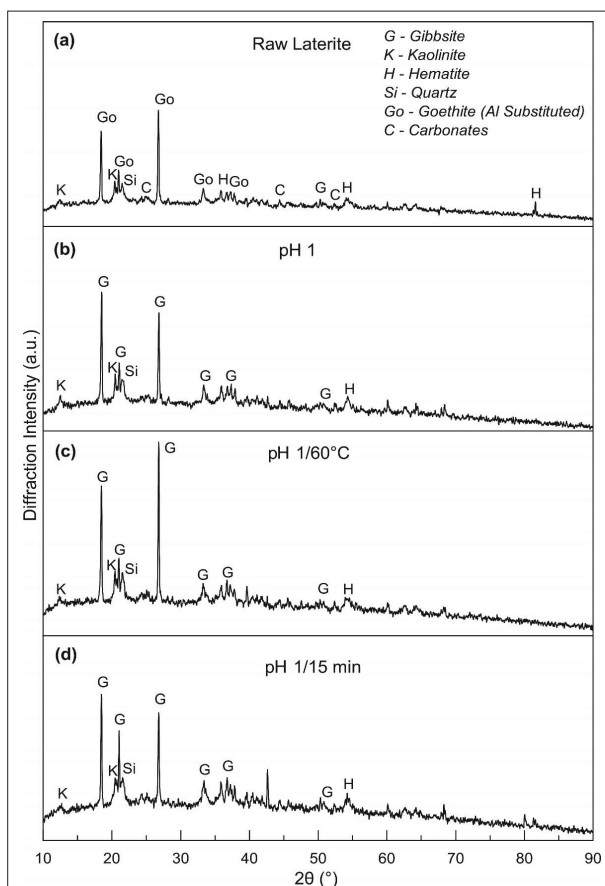


Figure 6: XRD spectra of (a) raw laterite, (b) acid leached (pH 1 solution), (c) acid leached and heated (pH 1/60°C), and (d) acid leached and sonicated (pH 1/15 min) samples

CONCLUSIONS

XRD results show goethite and hematite as main Fe-rich secondary minerals in Sri Lankan raw laterite. The Fe and Mn leaching efficiencies decrease with increase in pH from 1 to 5. The Cd leaching efficiency increase with pH from 1 to 10. Therefore, the Fe and Mn leaching efficiencies are controlled by hydrogen ion concentration. In contrast, Cd leaching was controlled by hydroxyl ion concentration. The Fe in the leachate obtained after treating at pH 1 showed a Fe enrichment factor of 17,690. Fe and Mn leaching efficiencies increased with temperature from 40 °C to 100 °C. However, pH 1, temperature 60 °C, and 15 min sonication time were determined as optimum industrial applicable conditions for Fe leaching from Sri Lankan laterite. Sonication for 15 min at 60 °C in pH of 1 was determined as the optimum condition for Mn leaching from Sri Lankan laterite, with an enrichment ratio of 2,695 in the leachate. The goethite found in laterite used in this study is (~Fe_{0.9}Al_{0.1})O(OH)) according to XRD analysis and this goethite would react with concentrated acid to form gibbsite and FeCl₃. Leaching Fe and Mn enhance the Al content present in laterite. Consequently, the upgraded laterite could be used in applications, such as an additive to adjust Al content in clinker during cement production. The leachate could be a potential source of Mn and Fe.

Acknowledgement

This research was supported by the Accelerating Higher Education Expansion and Development (AHEAD) Operation of the Ministry of Higher Education funded by the World Bank. The authors thank M.D. Nilantha, Sandun Wijerama, and Pradeep Ranathunga for assistance in laboratory work.

REFERENCES

- Ayanda O.S., Adekola F.A., Baba A.A., Fatoki O.S. & Ximba B.J. (2011). Comparative study of the kinetics of dissolution of laterite in some acidic media. *Journal of Minerals and Materials Characterization and Engineering* **10**(15): 1457–1472.
DOI: <https://doi.org/10.4236/jmmce.2011.1015113>
- Çetintaş S. & Bingöl D. (2020). Performance evaluation of leaching processes with and without ultrasound effect combined with reagent-assisted mechanochemical process for nickel recovery from laterite: Process optimisation and kinetic evaluation. *Minerals Engineering* **157**(01): 106562.

- DOI: <https://doi.org/10.1016/j.mineng.2020.106562>
- Cornell R.M. & Giovanoli R. (1993). Acid dissolution of hematites of different morphologies. *Clay Minerals* **28**(02): 223–232.
DOI: <https://doi.org/10.1180/claymin.1993.028.2.04>
- Cornell R.M., Posner A.N.M. & Quirk J.P. (1975). The complete dissolution of goethite. *Journal of Applied Chemistry and Biotechnology* **25**(09): 701–706
DOI: <https://doi.org/10.1002/jctb.5020250909>
- Dahanayake K. (1982). Laterites of Sri Lanka - a reconnaissance study. *Mineralium Deposita* **17**(02): 245–256.
DOI: <https://doi.org/10.1007/BF00206474>
- Dissanayake C.B. (1980). Mineralogy and chemical composition of some laterites of Sri Lanka. *Geoderma* **23**(02): 147–155.
DOI: [https://doi.org/10.1016/0016-7061\(80\)90016-6](https://doi.org/10.1016/0016-7061(80)90016-6)
- Dissanayake D.M.S.N., Mantilaka M.M.M.G.P.G., Paliawadana T.C., Chandrakumara G.T.D., De Silva R.T., Pitawala H.M.T.G.A., Nalin de Silva K.M. & Amaratunga G.A.J. (2019). Facile and low-cost synthesis of pure hematite (α -Fe₂O₃) nanoparticles from naturally occurring laterites and their superior adsorption capability towards acid-dyes. *RSC Advances* **9**(37): 21249–21257.
DOI: <https://doi.org/10.1039/C9RA03756J>
- Fan R. & Gerson A.R. (2011). Nickel geochemistry of a Philippine laterite examined by bulk and microprobe synchrotron analyses. *Geochimica et Cosmochimica Acta* **75**(21): 6400–6415.
DOI: <https://doi.org/10.1016/j.gca.2011.08.003>
- Gleeson S.A., Herrington R.J., Durango J., Velásquez C.A. & Koll G. (2004). The mineralogy and geochemistry of the Cerro Matoso SA Ni laterite deposit, Montelíbano, Colombia. *Economic Geology* **99**(06): 1197–1213.
DOI: <https://doi.org/10.2113/gsecongeo.99.6.1197>
- Goswami R.K. & Mahanta C. (2007). Leaching characteristics of residual lateritic soils stabilised with fly ash and lime for geotechnical applications. *Waste Management* **27**(04): 466–481.
DOI: <https://doi.org/10.1016/j.wasman.2006.07.006>
- Heiri O., Lotter A.F. & Lemcke G. (2001). Loss on ignition as a method for estimating organic and carbonate content in sediments: reproducibility and comparability of results. *Journal of Paleolimnology* **25**(01): 101–110.
DOI: <https://doi.org/10.1023/A:1008119611481>
- Herath J.W. & Pathirana H.C.N.C. (1983). Genesis and constitution of Sri Lanka laterites. *Journal of the National Science Council of Sri Lanka* **11**(02): 277–292.
DOI: <http://doi.org/10.4038/jnsfsr.v11i2.8390>
- Ilyas S., Srivastava R.R., Kim H., Ilyas N. & Sattar R. (2020). Extraction of nickel and cobalt from a laterite ore using the carbothermic reduction roasting-ammoniacal leaching process. *Separation and Purification Technology* **232**: 115971.
DOI: <https://doi.org/10.1016/j.seppur.2019.115971>
- Kyllönen H., Pirkonen P., Hintikka V., Parvinen P., Grönroos A. & Sekki H. (2004). Ultrasonically aided mineral processing technique for remediation of soil contaminated by heavy metals. *Ultrasonics Sonochemistry* **11**(03–04): 211–216.
DOI: <https://doi.org/10.1016/j.ultsonch.2004.01.024>
- Li J., Xiong D., Chen H., Wang R. & Liang Y. (2012). Physicochemical factors affecting leaching of laterite ore in hydrochloric acid. *Hydrometallurgy* **129–130**(01): 14–18.
DOI: <https://doi.org/10.1016/j.hydromet.2012.08.001>
- Liu K., Chen Q., Hu H. & Yin Z. (2010). Characterisation and leaching behavior of lizardite in Yuanjiang laterite ore. *Applied Clay Science* **47**(03–04): 311–316.
DOI: <https://doi.org/10.1016/j.clay.2009.11.034>
- Maiti A., Basu J.K. & De S. (2012). Experimental and kinetic modeling of As(V) and As(III) adsorption on treated laterite using synthetic and contaminated groundwater: Effects of phosphate, silicate and carbonate ions. *Chemical Engineering Journal* **191**(01): 1–12.
DOI: <https://doi.org/10.1016/j.cej.2010.01.031>
- Mitra S., Thakur L.S., Rathore V.K. & Mondal P. (2016). Removal of Pb(II) and Cr(VI) by laterite soil from synthetic waste water: single and bi-component adsorption approach. *Desalination and Water Treatment* **57**(39): 18406–18416.
DOI: <https://doi.org/10.1080/19443994.2015.1088806>
- Mohapatra B.K., Jena S., Mahanta K. & Mishra P. (2008). Goethite morphology and composition in banded iron formation, Orissa, India. *Resource Geology* **58**(03): 325–332.
DOI: <https://doi.org/10.1111/j.1751-3928.2008.00065.x>
- Moutei L., Benbrahim Y., Bouih A., Labied S., Guedira T. & Benali O. (2018). The effect of the addition of alumina powder on the confinement properties of a cement mortar. In *MATEC Web of Conferences* **149**: 01055.
DOI: <https://doi.org/10.1051/mateconf/201814901055>
- Nasab M.H., Noaparast M., Abdollahi H. & Amoozegar M.A. (2020). Indirect bioleaching of Co and Ni from iron rich laterite ore, using metabolic carboxylic acids generated by *P. putida*, *P. koreensis*, *P. bilaji* and *A. niger*. *Hydrometallurgy* **193**(01): 105309.
DOI: <https://doi.org/10.1016/j.hydromet.2020.105309>
- Nayanthika I.V.K., Jayawardana D.T., Bandara N.J.G.J., Manage P.M. & Madushanka R.M.T.D. (2018). Effective use of iron-aluminum rich laterite based soil mixture for treatment of landfill leachate. *Waste Management* **74**(01): 347–361.
DOI: <https://doi.org/10.1016/j.wasman.2018.01.013>
- Patermarakis G. & Paspaliaris Y. (1989). The leaching of iron oxides in boehmitic bauxite by hydrochloric acid. *Hydrometallurgy* **23**(01): 77–90.
DOI: [https://doi.org/10.1016/0304-386X\(89\)90019-4](https://doi.org/10.1016/0304-386X(89)90019-4)
- Perks C. & Mudd G. (2019). Titanium, zirconium resources and production: a state of the art literature review. *Ore Geology Reviews* **107**(01): 629–646.
DOI: <https://doi.org/10.1016/j.oregeorev.2019.02.025>
- Persons B.S. (2012). *Laterite: Genesis, Location, Use*. Springer Science & Business Media, Germany.
- Pham T.D., Pham T.T., Phan M.N., Ngo T.M.V. & Vu C.M. (2020). Adsorption characteristics of anionic surfactant onto laterite soil with differently charged surfaces and application for cationic dye removal. *Journal of Molecular Liquids* **301**(01): 112456.
DOI: <https://doi.org/10.1016/j.molliq.2020.112456>

Rathore V.K., Dohare D.K. & Mondal P. (2016). Competitive adsorption between arsenic and fluoride from binary mixture on chemically treated laterite. *Journal of Environmental Chemical Engineering* 4(02): 2417–2430.

DOI: <https://doi.org/10.1016/j.jece.2016.04.017>
The Aluminium Association (2020). Available at <https://www.aluminum.org/industries/production/alumina-refining>, Accessed August 2020.